XVI International Conference on Durability of Building Materials and Components
DBMC 2023, China
K.F. Li and D.P. Fang (Eds)

Effects of Multi-scale Siliceous additives on Hydration and Microstructure of Hardened Cement Pastes

X.S. Zhang, Y.R. Zhang, J.H. Zeng and K. Wu

School of Civil Engineering, Beijing Jiaotong University, Beijing 100044, PR China,
21115063@bjtu.edu.cn (X.S. Zhang), yr.zhang@bjtu.edu.cn (Y.R. Zhang), 21121217@bjtu.edu.cn (J.H. Zeng), 20115060@bjtu.edu.cn (K. Wu)

Abstract. *Siliceous materials are commonly used in concrete with physical filling and higher pozzolanic reactivity, such as silica fume (SF) and nano-silica (NS). Investigations were conducted into the effects of SF, hydrophobic silica fume (HSF), and synthesized NS on the mechanical properties and microscopic characteristics of hardened cement pastes (HCPs). The surface of silica fume was hydrophobically modified using isooctyltriethoxysilane. Fourier infrared spectrometer (FTIR), X-ray diffractometer (XRD), and energy spectrometer (EDS) were used to evaluate the hydration, while mercury intrusion porosimetry (MIP) and scanning electron microscope (SEM) were used to analyze the pore structure and microscopic morphology of HCPs. The results demonstrated that HSF has better dispersion in cement pore solution. The addition of HSF exhibits the higher pozzolanic reactivity, weakens CH diffraction peaks, generates higher levels Q_3 C-S-H gels, and significantly lowers the Ca/Si ratio of C-S-H gels. Due to the hydrophobicity, HSF increases the volume of micro-pores in range of 10-100 nm, resulting in a decrease in strength. Compounding HSF and NS further weakens the CH diffraction peak, decreases the Ca/Si ratio of C-S-H gels, and reduces the micro-pore volume to refines the pore structure.*

Keywords: *Hydrophobic silica fume, Cement hydration, Pore structure, Microstructure.*

1 Introduction

Silica fume (SF) is widely used as a highly reactive mineral admixture in cementitious materials. Silica fume, consisting of amorphous spherical SiO_2 particles, is able to play a physical filling role while generating C-S-H gels by pozzolanic reaction with cement hydration product CH (Huang et al. 2022). However, silica fume has a huge specific surface area and strong van der Waals forces between SiO_2 particles, which leads to the formation of silica fume agglomerates easily and difficult to disperse in cementitious materials, limiting the filler effect and pozzolanic effect. The main ways to reduce the degree of silica fume agglomeration include physical dispersion and chemical modification (Mitchell et al. 1998). Common physical dispersion methods include mechanical stirring, ball milling and ultrasonic dispersion; however, physically dispersed silica fume particles are prone to re-agglomeration in cement slurry solutions, so some scholars have proposed chemically modified dispersion methods, and

commonly used dispersants are calcium hydroxide, anionic water-reducing agents and anionic polymers (Baltazar et al. 2017, He et al. 2022, Jeong et al. 2020, Jinping et al. 2006, Lei et al. 2016, Xu et al. 1999, Zou et al. 2022). Silane, as a commonly used dispersant, can be modified to improve the dispersibility of silica fume using a simple treatment (Baltazar et al. 2017, Jeong et al. 2020, Xu et al. 2000, Baltazar et al. 2017). Hydrophobic silica fume (HSF) has good rheological properties, reduces plastic viscosity and yield stress, and has less effect on flexural strength and compressive strength. NS, as a powdered siliceous material with higher pozzolanic reactivity than silica fume and particle size less than 100 nm, not only has pozzolanic effect and good filling effect, but also has microcrystalline nucleation effect, which can refine the pore structure and improve the strength and durability of cementitious materials. Yan-Sheng Wang (Wang et al. 2020) found that nano-silica and silica fume synergize in activity and nucleation, making the hydration products significantly more and more dense in both early and late stages; meanwhile, nano-silica and silica fume synergize in size, making the concrete denser. However, the effect of synergistic silica materials at different scales on the hydration properties and microstructure of cementitious materials is still unclear.

This article compares the differences in properties between ordinary silica fume and modified silica fume through particle size analysis and Fourier transform infrared spectroscopy (FTIR). The effects of silica fume, modified silica fume, and co-doping with NS on the hydration properties of cementitious materials were studied using isothermal calorimetry, X-ray diffraction (XRD), and FTIR. The impact of SF, HSF, and co-doping with NS on the microstructure of cementitious materials was investigated using MIP and SEM-EDS. The study systematically explores the influence of micro-nano silica materials on the microscopic characteristics of cement-based materials.

2 Materials and Experimental Methods

2.1 Materials

Common silica fume and hydrophobic modified silica fume provided by Beijing Maple, P.I 42.5 cement produced by Fushun Cement Co., nano-SiO_2 with purity and average particle size of 99.5% and 50 nm respectively, superplasticizer provided by Beijing Maple and homemade deionized water were used.

To clarify the properties of SF and HSF, this study employed a laser particle size analyzer, X-ray diffraction (XRD), and Fourier transform infrared spectroscopy (FTIR) to characterize the physical and chemical properties of HSF. The British Malvern Nano ZS90 instrument was used to test the particle size distribution of SF and HSF in dispersing fluids including deionized water and clear solution of cement slurry, as shown in Figure 1(a). When deionized water was used as the dispersing fluid, the particle size distribution curve of HSF exhibited a leftward shift compared to SF, indicating that HSF has smaller particle size distribution. When SF and HSF

were dispersed in a pore solution, the particle size distribution curve shifted to the right. However, the degree of curve shift was less pronounced for HSF compared to SF. This suggests that HSF not only exhibits good dispersibility in water but also in freshly mixed cement slurry.

Ultima IV X-ray diffractometer was used to investigate the physical morphology of two types of silica fume. The scanning range was from 5° to 70° with a step size of 0.02° and duration of 0.4s/step. The results as Figure 1(b), show that both SF and HSF exhibit an amorphous structure without the presence of other substances. FTIR was conducted using the Thermo Scientific Nicolet iS10 spectrometer. The spectral range for FTIR analysis was set from 4000 to 400 cm^{-1}. The results are shown in Figure 3, indicating that both SF and HSF exhibit characteristic peaks of Si-O-Si antisymmetric and symmetric stretching vibrations around 1028 cm^{-1}, 786 cm^{-1}, and 425 cm^{-1}. In addition, HSF shows an additional C-H stretching absorption peak at 2927 cm^{-1}, suggesting that the modified material has undergone surface and chemical bonding with the silica fume particles.

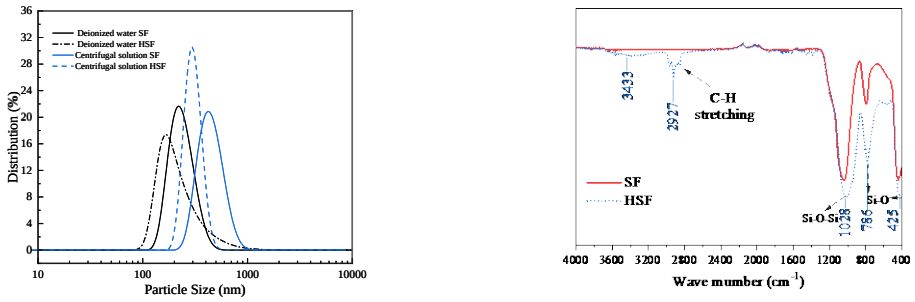

(a) particle size distribution (b) FTIR spectra

Figure 1. Comparison of properties between silica fume and hydrophobic silica fume

2.2 Specimen Preparation

The water-cement ratio of the cement paste was 0.35. To study the effect of hydrophobic silica fume on the properties of hardened cement paste, silica fume and hydrophobic silica fume were selected to replace 10 wt% cement; to evaluate how the performance of bulk cement paste may be affected as a result of the utilization of nano- and micro- silica admixtures, SF or HSF was compounded with NS at a mass ratio of 10:1, and 11 wt% cement was replaced by equal masses. Mixture proportions of cement-based materials is shown in Table 1.

Table 1. Mixture proportions of cement-based materials (mass%)

Type	Cement (%)	SF (%)	HSF (%)	NS (%)	w/b	Superplasticizer (%)
Blank	100				0.35	0.05
SF10	90	10			0.35	0.27

HSF10	90		90		0.35	0.12
SF10NS1	89	10		1	0.35	0.38
HSF10NS1	89		10	1	0.35	0.19

The superplasticizer was dissolved in water, followed by the addition of the SF, HSF and NS and mixing for two minutes. After that, the cement was added to the mixer and mixed for two minutes. The homogeneously mixed cement pastes were poured into cylindrical molds (Φ=20 mm, h=100 mm) for molding and cured for 7 d and 28 d for microscopic property analysis.

2.3 Hydration Characteristics Test

(1) Isothermal calorimetry

The early hydration process was monitored using a TAM Air isothermal calorimeter from USA. Firstly, the mixture of deionized water and superplasticizer were placed in an ampoule. Then cement, SF, HSF, NS were put into the ampoules and rapidly stirred uniformly. After putting cement paste samples in every channel, the calorimetric evolution was collected in the following 72 h at 25 ℃.

(2) XRD

The target-anode of X-ray diffraction was copper, and the working voltage and electric current were 40 kV and 40 mA, respectively. The step size is 0.02°. Scanning pace and range were 0.40 s/step and 5–70°, respectively.

(3) FTIR described in 2.1 were used to study the effects of hydrophobic silica fume and mixed siliceous materials of different sizes on the hydration.

2.4 Microstructural Characterization

(1) Pore analysis

The pore structure in HCPs was determined by MIP. The cores of the specimens were cut into 10 mm × 5 mm circular pies and soaked pieces were placed in a vacuum drying oven for 24 h at 40 ℃. The analysis was carried out using MicroActive AutoPore V 9600.

(2) Microstructure examination

The morphologies of HCPs and element distributions of hydrates were obtained by SEM-EDS. The specimens sheared into 5 mm×5 mm×2 mm slices. After drying and gold spraying, the surface micromorphology of the samples was observed by secondary electron probe mode, and the elemental composition of the hydration products was detected by energy spectrometry.

3 Results and Discussion

3.1 Hydration Characteristics

3.1.1 Calorimetric measurement

The effects of 10% SF and HSF on the hydration heat are shown in Figure 2. The addition of 10% SF increased both the maximum rate and the acceleration of hydration heat release during the acceleration period. Inversely, 10% HSF significantly reduced the rate of heat release during the acceleration period. However, after 47 hours, the hydration heat release rate of HSF10 was higher than Blank and SF10, illustrating that HSF10 was conducive to enhancing the hydration rate after 47 hours.

SF exhibits strong pozzolanic activity, and reacts with water during the early stages of hydration, leading to an increase in the rate of heat release during the acceleration period. Silane may be the reason for the significant reduction of early hydration heat release rate of HSF. Silane not only inhibits cement hydration, but also the carbon chains on the surface of silane are not conducive to unleashing the pozzolanic effect owing to which prevent the diffusion of water and hydroxide ions towards the cement particles. However, As the hydration progresses, the pH of the matrix increases, causing Si-O bond breakage, which results in the detachment of silane from the surface of cement particles and allowing the cement particles to continue the pozzolanic reaction. In addition, hydrophobic cement particles have better dispersibility, leading to a higher hydration heat release rate compared to the Blank and SF10.

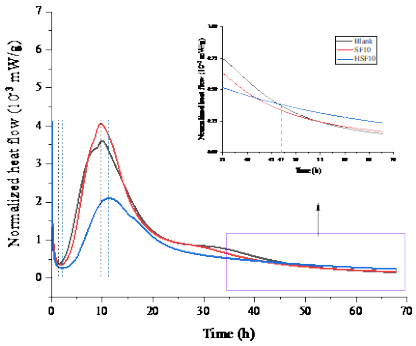

Figure 2. Effect of SF and HSF on hydration heat rate of cement

3.1.2 XRD

Based on XRD, the effects of SF, HSF, and the combined addition of NS on the unhydrated clinker minerals (C_2S and C_3S) and hydrated product (CH) in the HCPs were studied, as shown in Figure 3. At 7 days, the addition of 10% SF significantly weakened the CH diffraction peak, while it had a minor effect on the diffraction peaks of C_2S and C_3S. On the other hand, the addition of 10% HSF weakened both the CH diffraction peak and diffraction peaks of C_2S and

C_3S. Compared to the singly added SF and HSF at 10%, NS, when combined with SF and HSF, respectively strengthened and weakened the CH diffraction peak. At 28days, the reduction in the CH diffraction peak caused by HSF was more significant than that by SF, and the diffraction peaks of C_2S and C_3S were slightly decreased. These results indicate that SF can promote the pozzolanic reaction in the early hydration stage, while HSF exhibits more pronounced reactivity with pozzolanic reaction in the later stage of hydration.

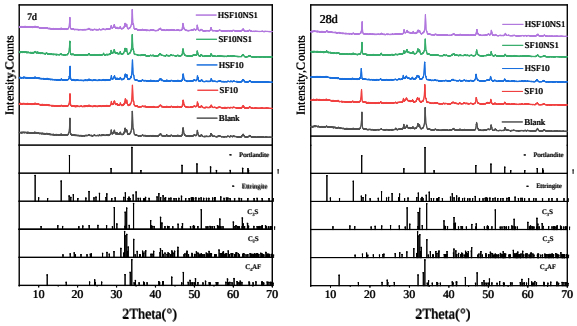

Figure 3. Qualitative phase analysis with ICSD reference patterns

3.1.3 FTIR

Fig.4 shows the effect of the compacting agent on the hydration properties of cementite was investigated by FTIR. 3644 cm^{-1} corresponds to the $Ca(OH)_2$ O-H stretching vibration peak; the O-H stretching vibration peak of adsorbed water is 3456 cm^{-1}; the absorption bands around 1110/1000/935/822 cm^{-1} correlate with the Si-O-Si of SiO_4 at n=4/3/2/1, respectively; 870 cm^{-1} corresponds to the C-O stretching vibration peak. stretching vibration.7d, SF10 significantly weakened the $Ca(OH)_2$ O-H stretching vibration peak, but HSF10 weakened to a lesser extent, indicating that the early SF pozzolanic activity is higher than HSF, which is consistent with the conclusion of TG-DSC and XRD analysis.

As shown in Fig. 6(b), SF10, HSF10, SF10NS1, and HSF10NS1 all significantly increased SiO_4 Si-O-Si stretching vibration peak. Due to the mutual overlap of the Si-O-Si absorption vibration peaks of SiO_4 in the range of 748~1333 cm^{-1} and the C-O absorption vibration peaks, for quantitative calculations, the absorption vibration spectra in this region were deconvoluted to identify individual peaks and calculate the peak areas, which represent the corresponding substance contents, and the areas were normalized, and the results are shown in Tab. 3.

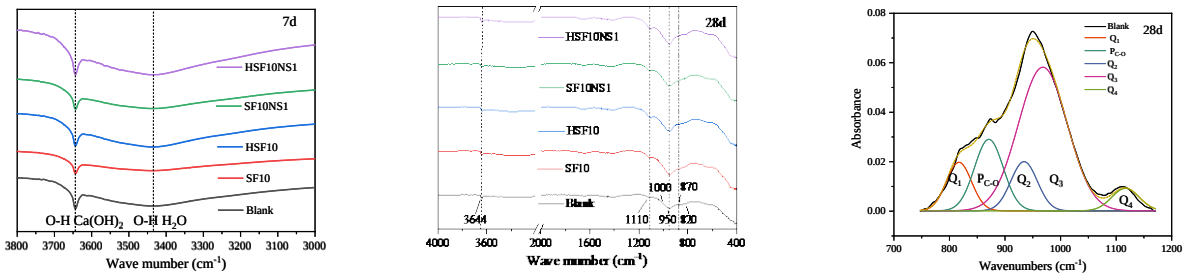

(a) 7 d (b) 28 d (c) 748~1333cm^{-1}

Figure 4. FTIR spectrum measured for the HCPs and with the four bands used to fit this spectrum

The Q_3 content was increased from 10.55% to 13.36% with 10% HSF, and the compounding of NS mainly increased the Q_2 content and slightly increased the Q_3 content. It indicates that HSF is beneficial to improve the C-S-H polymerization, and the synergistic effect of HSF and NS can promote cement hydration while slightly promoting the occurrence of pozzolanic reaction.

Table 2. Normalized area indices at different ages

	A_{SiO4}	Q_1	P_{C-O}	Q_2	Q_3	Q_4
Blank	13.09	16.74%	9.83%	33.60%	29.28%	10.55%
SF10	21.98	14.79%	9.89%	39.76%	27.43%	8.12%
HSF10	22.98	12.15%	4.96%	37.67%	31.87%	13.36%
SF10NS1	24.07	15.18%	8.14%	38.57%	26.15%	11.95%
HSF10NS1	27.22	12.95%	4.97%	30.56%	37.95%	13.57%

3.2 Pore Structure

3.2.1 MIP

Tab.3 shows the pore size distribution of HCPs at 28 days. The addition of silica fume increased the volume of gel pores (≤10 nm), small capillary pores (10-100 nm), and large capillary pores (>100 nm), as well as the porosity and pore size distribution, while decreasing the average pore diameter. Modified silica fume exhibited a similar effect, with a more significant increase in the content of gel pores and capillary pores. The co-addition of SF/HSF and NS further increased the volume of gel pores, while reducing the volume of small capillary pores.

SF, HSF increases the gel pore volume mainly due to the pozzolanic reaction of active SiO_2 in silica fume to generate C-S-H gels, the better dispersed HSF has a stronger pozzolanic effect in hydration, but due to the water-repellent effect of silane on the surface of modified silica fume, resulting in an increase in the water-gel ratio of the slurry and an increase in capillary pore volume.

Table 3. The characteristic parameters of pore structure of HCPs

	1-10nm (cm^3/g)	10-100nm (cm^3/g)	＞100nm (cm^3/g)	Average pore diameter（nm）	Porosity（%）
Blank	2.02	7.24	0.34	13.79	18.06
SF10	2.78	7.30	0.63	11.80	20.59

HSF10	3.50	8.65	0.52	11.98	22.11
SF10NS1	3.47	5.62	0.59	9.37	17.62
HSF10NS1	3.77	8.15	0.58	11.44	21.67

3.2.2 SEM-EDS

Fig.5 demonstrates the effects of SF, HSF and NS on the microstructure of HCPs by SEM. As shown in Fig.5 (a)-(b), silica fume is difficult to disperse in the cement paste, resulting in a large number of dense agglomerates in the matrix. However, modified silica fume has almost no agglomerates in the HCPs, indicating that modified silica fume has good dispersibility in the cement paste.

As shown in Fig.5(c), a layer of small particle-like gels adhere to the surface of silica fume, which is C-S-H gel formed by the pozzolanic reaction of silica fume adsorbing free CH on the surface of silica fume. After adding 1% NS, the surface of the silica fume was almost completely covered by the C-S-H gels, and the stacking of gel was dense, which confirmed the assumption of pore structure. As shown in Fig. 5(d), the modified silica fume surface is covered with a more compact C-S-H hydrated calcium silicate gel.

Ca/Si atom ratios of C-S-H gel in HCPs were analyzed semi-quantitatively by detected energy spectral analysis and calculated by linear fitting, as shown in Figure 5(e). SF10 and HSF10 can significantly reduce the Ca/Si atom ratio, which were 1.7 and 1.64, respectively, demonstrating that the modified silica fume is more conducive to enhance the polymerization degree of C-S-H gel. Ca/Si atom ratios are lower in SF10NS1 than SF10, and similar trends are observed for HSF10, owing to the synergistic effect.

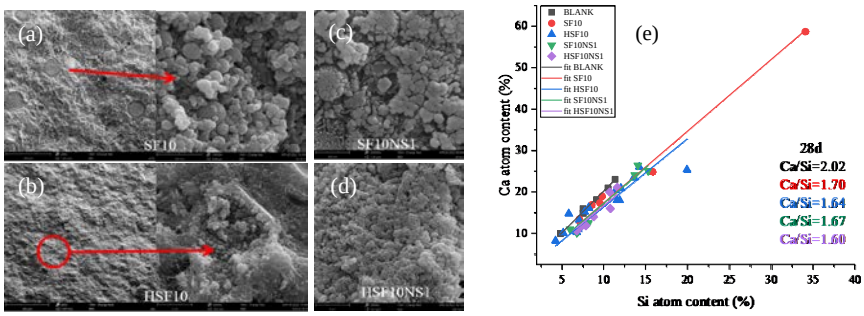

Figure 5. The SEM images of HCPs and Ca/Si atom ratios of the gel in HCPs

4 Conclusions

In this article, the properties of ordinary silica fume and modified silica fume were compared. The effects of the two types of silica fume and the co-doping of NS on cement hydration and microstructure were systematically studied, the following conclusions can be drawn.

- Compared to SF, HSF exhibits better dispersibility in deionized water and cement pore solution. FTIR spectra displays C-H and Si-O-Si are grafted onto the surface of silica fume by Silane modification.
- SF undergoes pozzolanic reaction in the early stage of hydration, increasing the rate of heat release. On the contrary, HSF reduces the rate of heat release in the early stage of hydration, but HSF is beneficial for increasing the rate of heat release after 47 hours. The CH absorption peak of HSF is higher than that of SF in the early stage of hydration, and HSF can significantly increase the content of Q3.
- Both SF and HSF can significantly increase the content of gel pores in HCPs at age of 28 days, but also increase the volume of capillary pores. Co-doping SF or HSF with NS are beneficial for increasing the gel pores while reducing the volume of small capillary pores.
- SF exists mostly in the form of agglomerates in cementitious materials, while HSF has significantly reduced agglomerate quantity owing to the excellent dispersibility. Co-doping HSF with NS promotes the formation of dense C-S-H gel and significantly reduces the Ca/Si atom ratios.

References

Huang, J., Zhao, Y., Wang, X., Manuka, M., Hu, H., Ding, Z., Yin, H., and Ma, B. (2022). *Dispersing silica fume in cementitious materials by silane copolymerized polycarboxylate Superplasticizer: On the role of dispersion effectiveness as a function of silane concentration*. Construction and Building Materials, 326, 126832.

Mitchell, D. R. G., Hinczak, I., Day, and R. A. (1998). *Interaction of silica fume with calcium hydroxide solutions and hydrated cement pastes*. Cement and Concrete Research, 28(11), 1571-1584.

Baltazar, L., Henriques, F., Rocha, D., and Cidade, M. (2017). *Experimental Characterization of Injection Grouts Incorporating Hydrophobic Silica Fume*. Journal of Materials in Civil Engineering, 29,

He, Y., Liu, S., Zhang, X., Hooton, R. D., Ji, T., and Shen, J. (2022). *Synthesis and dispersing properties of organosilane-modified superplasticiser in cement–silica fume composite binder*. Advances in Cement Research, 34(4), 139-150.

Jeong, Y., Kang, S., Kim, M. O., and Moon, J. (2020). *Acceleration of cement hydration from supplementary cementitious materials: Performance comparison between silica fume and hydrophobic silica*. Cement and Concrete Composites, 112, 103688.

Jinping, O., Tiejun, L., and Jiahe, L. (2006). *Analysis of the damping behavior and microstructure of cement matrix with silane-treated silica fume*. Journal of Wuhan University of Technology-Mater. Sci. Ed., 21(2), 1-5.

Lei, D., Guo, L., Sun, W., Liu, J., Shu, X., and Guo, X. (2016). *A new dispersing method on silica fume and its influence on the performance of cement-based materials*. Construction and Building Materials, 115, 716-726.

Xu, Y., and Chung, D.D.L. (1999). *Improving the workability and strength of silica fume concrete by using silane-treated silica fume*. Cement and Concrete Research, 29(3), 451-453.

Zou, D., Wang, D., Zhang, S., and Li, H. (2022). *Influence of self-dispersing particles on workability, hydration*

and strength of ultra-high-performance concrete. Construction and Building Materials, 326, 126727.

Xu, Y., and Chung, D.D.L. (2000). *Improving silica fume cement by using silane*. Cement and Concrete Research, 30(8), 1305-1311.

Baltazar, L., Henriques, F., Rocha, D., and Cidade, M. (2017). *Experimental Characterization of Injection Grouts Incorporating Hydrophobic Silica Fume*. Journal of Materials in Civil Engineering, 29(10), 4017167.

Wang, Y., Xu, Z., Wang, J., Zhou, Z., Du, P., and Cheng, X. (2020). *Synergistic effect of nano-silica and silica fume on hydration properties of cement-based materials*. Journal of Thermal Analysis and Calorimetry, 140(5), 2225-2235.